Luminescence in Lead Tungstate Hollow Nano Tubes

[1]M.Srinivas, [2]D.Tawde, [3]Verma Vishwnath, [4]Nimesh Patel and [5]K.V.R.Murthy

[1,2,3,4] Luminescent Materials Laboratory, Physics Department, Faculty of Science, The M. S. University of Baroda, Vadodara-390002, India;

[5]Display Materials Laboratory, Applied Physics Department, Faculty of Technology and Engineering, The M. S. University of Baroda, Vadodara – 390001 India.

E-mail: mnsmsu@gmail.com , dharmendra_tawde@yahoo.com, drmurthykvr@yahoo.com

Abstract:- ***$PbWO_4$ nanostructures synthesized via Low Temperature Hydrothermal (LTH) method at different pH without using any surfactant. As-synthesized samples were characterized by X-ray diffraction technique (XRD), Transmission Electron Microscopy (TEM) and Photoluminescence (PL). XRD spectra reveal that $PbWO_4$ synthesized at different pH of reaction solution was highly crystalline, single phase and indexed to a pure tetragonal stolzite phase with space group $I4_1/a$. Hallow Nano particles (HNPs) and Hollow Nano tubes (HNTs) of $PbWO_4$ were obtained at 7pH.. HNPs with 20-40 nm average diameter and HNTs having outer diameter approximately 12.37 nm and length around 80-170 nm were obtained. The formation of HNTs of $PbWO_4$ due to the Kirkendall effect and have nanofluidic application in nano optical devices. Room Temperature Photoluminescence spectra recorded at 254 nm excitation wavelength shows broad luminescence emission in blue-green region. PL spectra was fitted with four individual Gaussian peaks having peak positions for peak I (365 nm), peak II (395 nm), peak III (459 nm) and peak IV (500nm).***

Key Words: Low Temperature Hydrothermal (LTH), X-ray diffraction technique (XRD), Transmission Electron Microscopy (TEM) Photoluminescence (PL), Hollow Nano Tubes (HNTs)

INTRODUCTION

In the present paper, we report the template free hydrothermal route for the formation of Hollow Nanotubes (HNTs) for the first time in case of $PbWO_4$. After the discovery of hollow carbon nanoparticles (i.e.C_{60}) in 1985 by Smalley and co-workers [1] and hollow carbon nanotubes in 1991 by Iijima [2], and the subsequent discovery of fullerene-like WS_2 nanotubes and nanoparticles (NP) by Tenne et al.,[3-4] a great deal of attention has been devoted to the synthesis and characterization of hollow inorganic nanotubes. Lead tungstate ($PbWO_4$) is an important inorganic scintillating material of the tungstate family with tetragonal scheelite and monoclinic raspite type structure. $PbWO_4$ crystal is most attractive for its high-energy particle physics applications because of its high density (8.3 g cm^{-3}), and good luminescence properties. Recently many efforts have been made to the controlled synthesis of $PbWO_4$ micro- and nanocrystals. Various morphologies, including microspheres [5] nanobelts [6-7] helical structures [8] hollow nanospindles [9] quasi-octahedra [10] polyhedral [11] micro- crystals [12-13] have been achieved .

EXPERIMENTAL

Analytical Reagent grade Lead Chloride ($PbCl_2$) and Sodium tungstate ($Na_2WO_4 \cdot 2H_2O$) supplied by Alfa Aesar . Distilled water was used as solvent for the preparation of required solutions. In order to synthesize $PbWO_4$ at different pH, pH of distilled water was set to 3 by adding Acetic acid (Glacial) (CH_3COOH) and subsequently increased up to 11 by adding Sodium Hydroxide (NaOH). 30 ml solution of 0.01 M concentration of $PbCl_2$ was initially prepared by dissolving 0.08343 g of $PbCl_2$ in a beaker containing 30ml distilled water with continuous stirring on a temperature controlled magnetic stirrer. Similarly 30 ml solution of 0.01 M (0.0989 g) concentration of Na_2WO_4 was added into $PbCl_2$ solution and precipitates of $PbWO_4$ were obtained. The resulting precursor solution was transferred to Teflon lined stainless steel autoclave having 90 ml capacity filled 80%. The autoclave was maintained at a temperature of 130 °C for 4 h and then air cooled to room temperature. The precipitates obtained were washed and filtered several times with distilled water by using Wattman fine filter paper to remove salt which is produced during reaction and lastly with absolute ethanol. To remove water content obtained white powder was dried in vacuum Oven at 80°C for 2h. Three samples were synthesized by this method at 3, 7 and 11pH.

Powder X-ray diffraction (XRD) patterns were recorded with a Japan Rigaku D8 advance diffractometer using Cu K_α radiation (0.15406 nm). The particle size and surface morphology of the polycrystalline powders were

observed by Transmission Electron Microscopy (TEM, Tecnai 20 G2 PHILIPS, Holland made). The PL studies were made by using Shimadzu spectrofluorophotometer (1503 R-PC) at room temperature with a xenon lamp as excitation source.

RESULTS AND DISCUSSION

X-ray Diffraction Analysis igure 2 shows XRD spectra of $PbWO_4$ [14], synthesized at different pH of 3, 7 and 11. The XRD data files for these samples were analysed with by Powder-X software and Indexed images are shown as below.

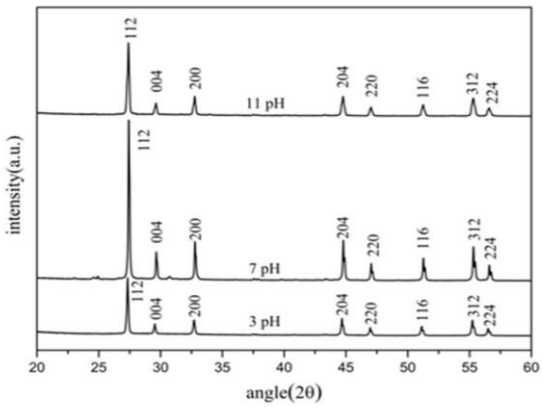

Figure 1 XRD spectra of $PbWO_4$ prepared at different pH.

The XRD reflections that $PbWO_4$ synthesized at different pH having a single phase. All the reflection peaks can be completely indexed to a pure tetragonal stolzite phase of $PbWO_4$ with space group $I4_1/a$. Formation of Tungstic acid ($H_2WO_4.nH_2O$), tungsten oxide hydrates ($WO_3.nH_2O$) and unwanted impurities of Na_2WO_4 were not observed from XRD. The strong and sharp peaks indicate that $PbWO_4$ obtained at different values of pH were highly crystallized and structurally ordered at long-range. Comparing XRD spectra of these samples, presented in fig.2 it is noted that relative intensity of peaks varies significantly, which indicates that crystallinity also varies with pH. $PbWO_4$ prepared at 7pH and 11pH shows good crystallization than one made at 3pH. This result shows that different pH promotes the formation of crystalline $PbWO_4$ nanostructures at low temperature of synthesis.

According to Jun Geng et al. [15], 5-9 pH range is optimal for the production of $PbWO_4$ with different morphologies. If the pH value is higher than 11, another complex, $Pb(OH)_x^{2-x}$, was formed due to the high concentration of OH^- and the strong complex nature between Pb^{2+} and OH^-. The result presented in this paper shows that $PbWO_4$ nanomaterials with good crystallinity can be formed even at 11pH and thus optimal pH range is extended to 3-11 pH.

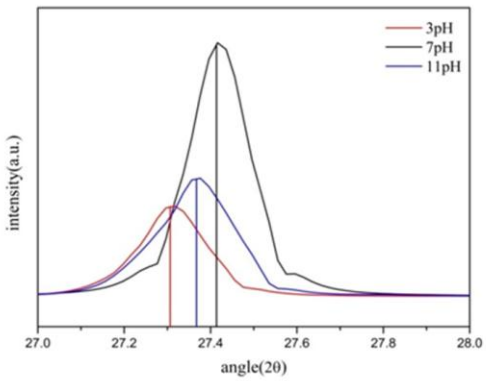

Figure 2 Shift of (112) reflection peak of $PbWO_4$ prepared at different pH.

It is seen from the figure that (112) peak for sample prepared at 3 pH is at lowest angle and that for sample prepared at 7pH is at highest angle a small shift in peak position is observed. According to Bragg's equation, the shift towards higher angle of reflection peaks suggests, that the cell parameters of as-synthesized samples continuously decreases. By using Powder-X software, the calculated lattice parameters for all three samples presented in Table-1, the average crystallite size had been estimated by the Scherrer's equation using the full width at half maximum (FWHM) for the intense peak (1 1 2). The average crystallite size was calculated using the Debye-Scherrer formula given in the literature [16].

pH	Phase	Lattice Parameter (Å)			Volume $(Å)^3$	Average Crystallite size (nm)
		a	b	c		
3	stolzite	5.4614	5.4614	12.046	359.29	40.75
7	stolzite	5.4590	5.4590	12.042	358.85	44.75
11	stolzite	5.4598	5.4598	12.045	359.05	35.45

Table 1: Summary of phase identified, lattice parameters, unit cell volume and average crystallite size of $PbWO_4$ prepared at different pH.

TRANSMISSION ELECTRON MICROSCOPY (TEM)

In order to analyze size and surface morphology of $PbWO_4$ sample prepared at 7pH show excellent photoluminescence properties. TEM images of $PbWO_4$ prepared at 7pH shown in Figure 3(a-b), respectively.

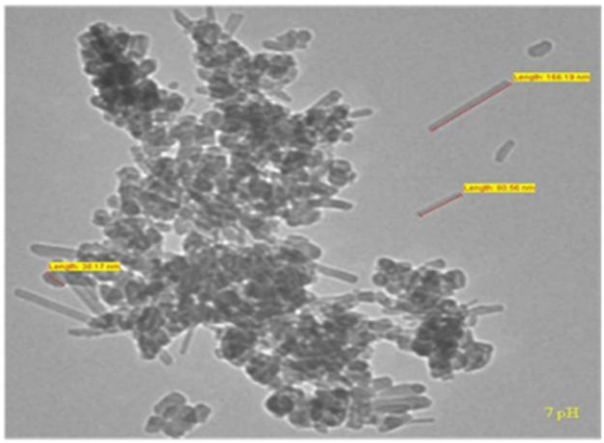

Figure 3(a)

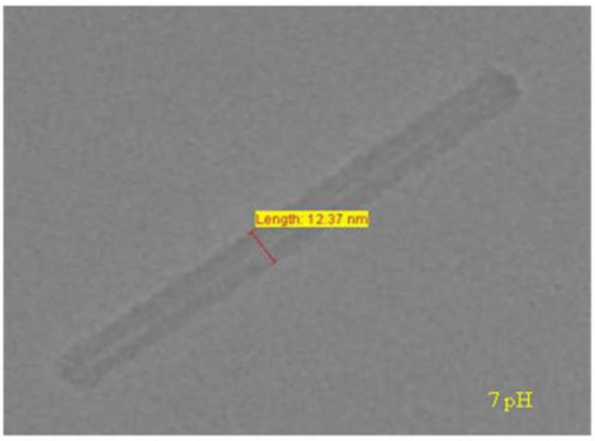

Figure 3(b)

The sample obtained at 7pH shows agglomerated hollow nanotubes (HNTs) of $PbWO_4$ as shown in Figure 3(a-c). HNTs have outer diameter approximately 12.37 nm and length around 80-170 nm.

roposed Mechanism of formation of Hollow Nanostructures of $PbWO_4$

Aldinger was the first to study the hollowing of spherical particles induced by the Kirkendall effect early in 1974 [17]. Only one author Fan Dong [18] was reported the formation of hollow nano particles of $PbWO_4$ synthesized by ultrasonic spray pyrolysis method using citric acid surfactant. Formation of hollow nanoparticles (HNPs) can be explained on the basis of Kirkendall counter diffusion effect shown in Figure 4.

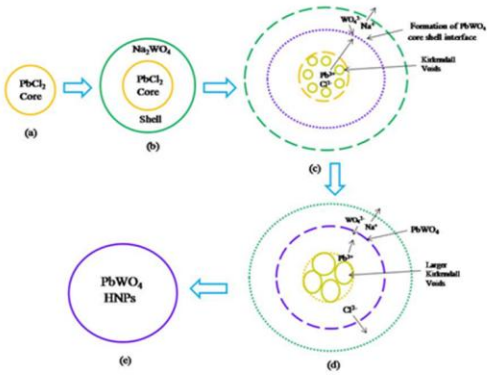

Figure 4 Schematic diagram showing proposed mechanism for formation of $PbWO_4$ Hollow Nano Particles by Process A.

This is a typical ternary compound reaction. In this reaction two reagents $PbCl_2$ (compound A) and Na_2WO_4 (compound B) sacrifice themselves to produce HNPs of $PbWO_4$ (compound AB). We propose that there are two possible ways, Process A and Process B. Both processes are based on Core/Shell model with a difference, only in Core and Shell Compound. Process A is shown schematically in Figure 4. In the Process A, (a) initially agglomerated $PbCl_2$ molecules behave as a Core and Na_2WO_4 molecules gathered around it and form a shell shown in (b). Pb^{2+} ions from the core, diffuse to the shell side and WO_4^{-2} ions from the shell diffuse to the core side. By this way Kirkendall diffusion will takes place in the form of two way mass transfer (Wagner counter diffusion) i.e. between core and shell compounds. Thus the product $PbWO_4$ formed at core/shell interface site. Simultaneously Na^+ ions move and react with Cl^- ions outer side to form NaCl which will dissolve in aqueous solution. At the same time small isotropic voids are formed in core contains only Cl^- ions shown in (c). Small Kirkendall voids merge into each other and forms larger cavities. If gaps are present at the core/shell interface would appear during the growth, Cl^- ions escape from these gaps and direct dissolution of Cl^- ions is taking place in solution phase shown in (d), The final product of $PbWO_4$ Nanoparticles shown in (e). HNPs of $PbWO_4$ form by Process B in a similar way with Na_2WO_4 as Core and $PbCl_2$ as Shell.

HOLLOW NANOTUBES (HNTS) OF $PBWO_4$

Formation of $PbWO_4$ Hollow Nano Tubes (HNTs) have not been reported yet, hence the results presented are first to report the synthesis of HNTs. Formation of tubular Hollow structures based on Kirkendall effect was reported in ref [19]. The Kirkendall-based formation route of $PbWO_4$ HNPs can also been extended to tubular structures. The nanotubes have one more degree of freedom and allow material to transport along the longitudinal axes. Elimination of the Cl^- from the core is taking place via open ends of Nanotubes makes them hollow. .

Photoluminescence (PL) analysis

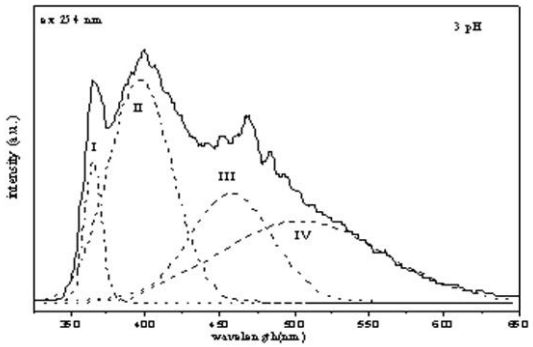

Figure 5 (a)

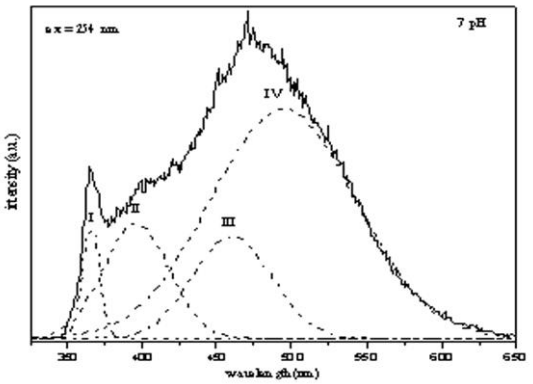

Figure 5 (b)

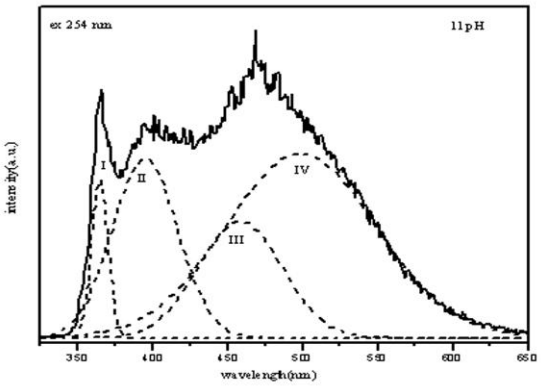

Figure 5 (c)

Figure 5 PL emission of $PbWO_4$ synthesized at different pH excited with 254 nm

Figure 5 (a-c) shows room temperature photoluminescence spectra of $PbWO_4$ prepared at three different (3, 7 and 11) pH of reaction solution excited with 254 nm wavelength. It shows broad blue-green emission in visible region with a central peak (400 nm) surrounded by two broad shoulder peaks (375 and 475 nm). The position of the emission peaks remained almost unchanged for all samples of 3, 7 and 11pH. It is well known that the luminescence spectrum of $PbWO_4$ is composed of two main bands; the ''blue'' one peaking around 420 nm and the ''green'' one peaking between 490 to 540 nm. The formation of two defects are mainly $(WO_4)^{-2}$ defects and another defect based on WO_3 center, mainly responsible for the complex character of $PbWO_4$ emission. The blue luminescence is an intrinsic feature of $PbWO_4$, and is generally ascribed to the radiative decay of a self-trapped exaction that locates on the regular $(WO_4)^{-2}$ group. The green luminescence is of extrinsic origin and ascribed to a defect based WO_3 center possibly with F center. The presence of four Gaussian peaks indicates the excited states of emission centres and degenerated. In order to investigate detailed parameters about luminescence properties of $PbWO_4$, emission spectra were fitted using four individual Gaussian peaks and for peak I (365 nm), peak II (395 nm), peak III(459 nm) and peak IV (500nm) to achieve good agreement with the experimental data. Variation in position of Gaussian peaks and their intensities are also shown in Table 2.

pH	Gaussian peak I		Gaussian peak II		Gaussian peak III		Gaussian peak IV	
	wavelength (nm)	intensity (a.u.)	wavelength (nm)	intensity (a.u.)	wavelength (nm)	intensity (a.u.)	wavelength (nm)	intensity (a.u.)
3	365	20	397	30	458	15	505	12
7	365	48	396	50	460	44	494	97
11	365	39	395	44	458	29	499	45

Table- 2: Positions and intensity of Gaussian components of PL spectra of $PbWO_4$ prepared at different pH.

In PL spectrum the blue emission is attributed to the radiative recombination of STE localized in regular WO_4^{2-} complex of scheelite phase. Isolated WO_4^{2-} complex has tetrahedral symmetry T_d with ground state

configuration $(t_1)^6(e)^0$ [33,34]. Excited configuration $(t_1)^5(e)^1$ results four electronic states: two singlets and two triplets: $^1T_2 < ^1T_1 < ^3T_2 \cong ^3T_1$[35]. It is accepted that blue luminescence originates from the $^3T_2 \cong ^3T_1 \rightarrow ^1A_1$ [36]. Because of the symmetry lowering from T_d to C_{3v} due to the JT effect, the $^3T_1$ state splits into the $^3A_2$ and ^3E sublevels, and the $^3T_2$ state into the $^3A_1$ and ^3E sublevels [37]. We conclude that the Gaussian peak I, the Gaussian peak II and the Gaussian peak III may correspond to the radiative transitions from $^3A_1 \rightarrow ^1A_1$, $^3A_2 \cong ^3E \rightarrow ^1A_1$ and $^3A_2 \rightarrow ^1A_1$, respectively. Hence blue emission occurs from the lower lying triplet state split by Jahn-Teller interaction. The Gaussian peak IV ascribed to oxygen deficient irregular WO_3 neutral molecule.

According to XRD spectra, sample prepared at 7pH has highest crystallinity then prepared at 3pH and $PbWO_4$ prepared at 11 pH shows intermediate crystallinity. Crystallinity shows higher PL emission which can be seen from PL spectra (Figure 5). Luminescence intensity increased with increasing pH, over the range of 3-7 pH, implying that $PbWO_4$ (HNPs and HNTs) obtained at 7pH have much more luminescence intensity. PL intensity of blue Gaussian peaks is highest for sample prepared at 7pH (HNPs + HNTs), intermediate for sample prepared at 11pH

(Nanorods) and lowest for sample prepared at 3pH which indicates that $PbWO_4$ HNPs and HNTs have more regular lattice structure and uniform morphology compared to Nanorods.

CONCLUSIONS

$PbWO_4$ nanomaterials synthesized successfully via Low Temperature Hydrothermal (LTH) method at different pH without using any surfactant or templates. X-ray diffraction analysis (XRD), Transmission Electron Microscopy (TEM) and Photoluminescence (PL) spectra reveals that effect of pH on reaction system has great influence on structural and optical properties of $PbWO_4$. XRD spectra shows that $PbWO_4$ synthesized at different pH of reaction solution were highly crystalline, single phase and indexed to a pure tetragonal stolzite phase with space group $I4_1/a$. Hallow Nanoparticles (HNPs) and Hollow Nanotubes (HNTs) of $PbWO_4$ were obtained at 7pH. HNPs with 20-40 nm average diameter and HNTs having outer diameter approximately 12.37 nm and length around 80-170 nm were formed. We concluded that the formation of HNTs of $PbWO_4$ is due to the Kirkendall effect and may have nano fluidic application in nano optical devices. Room Temperature Photoluminescence spectra recorded at 254 nm excitation shows broad luminescence emission in blue-green region. Obtained PL spectra was fitted with four individual Gaussian peaks having peak positions for peak I (365 nm), peak II (395 nm), peak III(459 nm) and peak IV (500nm). PL spectra of nano-sized $PbWO_4$ crystallites are strongly relied on their morphology and crystallinity. Size-dependent emission of photoluminescence observed among these three products with different morphologies indicates that the sizes of these structures may be in quantum confinement regime.

REFERENCES

[1] H.W. Kroto, J. R. Heath, S. C. O'Brien, R. F. Curl, R. E. Smalley, Nature 1985, 318, 162.

[2] S. Iijima, Nature 1991, 354, 56.

[3] R. Tenne, L. Margulis, M. Genut, G. Hodes, Nature 1992, 360,444.

[4] L. Margulis, G. Salitra, R. Tenne, M. Talianker, Nature 1993, 365, 113.

[5] Q. Zhang, W. T. Yao, X. Y. Chen, L. W. Zhu, Y. B. Fu, G. B. Zhang, L. Sheng and S. H. Yu, Cryst. Growth Des., 2007, 7, 1423–1431.

[6] C. H. Zheng, C. G. Hu, X. Y. Chen, H. Liu, Y. F. Xiong, J. Xu, B. Y. Wan and L. Y. Huang, Cryst Eng. Comm, 2010, 12, 3277–3282.

[7] D.Tawde, M.Srinivas and K.V.R.Murthy, Phys. Status Solidi A, 1–5 (2011) / DOI 10.1002/pssa.201026554.

[8] B. Liu, S. H. Yu, L. J. Li, Q. Zhang, F. Zhang and K. Jiang, Angew. Chem., Int. Ed., 2004, 43, 4745–4750.

[9] J. Geng, J. J. Zhu, D. J. Lu and H. Y. Chen, Inorg. Chem., 2006, 45, 8403–8407.

[10 G. Z. Wang, C. C. Hao and Y. F. Zhang, Mater. Lett., 2008, 62, 3163–3166.

[11] J. Geng, J. J. Zhu and H. Y. Chen, Cryst. Growth Des., 2006, 6, 321– 326.

[12] F. F. Wang, C. S. Li and H. Tang, J. Alloys Compd., 2010, 490, 372– 376.

[13] J. H. Yang, C. H. Lu, H. Su, J. M. Ma, H. M. Cheng and L. M. Qi, Nanotechnology, 2008, 19(3), 035608.

[14] D Tawde et al. Int. J. Lum and its Appln, Vol. 3 (2013) 79 – 82.

[15] Jun Geng et al.,Crystal Growth & Design, Vol. 6, No.1, 2006.

[16] C. Suryanarayana, M.G. Norton, X-ray Diffraction: A Practical Approach, Plenum Press, New York, 1998.

[17] F. Aldinger, Acta Metal., 22, 923,1974.

[18] Fan Dong, Yu Huang, Shichun Zou, Jiang Liu,‡ and S. C. Lee J. Phys. Chem. C, Vol. 115, No. 1, 2011.

[19] Q. Li, R. M. Penner, Nano Lett., 5, 1720, 2005.

◈◈◈